Solar Energy Materials & Solar Cells 148 (2016) 87–98

Contents lists available at ScienceDirect

Solar Energy Materials & Solar Cells

journal homepage: www.elsevier.com/locate/solmat

PV panel single and double diode models: Optimization of the parameters and temperature dependence

Nicolas Barth [a,*], Raka Jovanovic [a], Saïd Ahzi [a,b], Mohammad A. Khaleel [a,b]

[a] Qatar Environment and Energy Research Institute (QEERI), Hamad bin Khalifa University, Qatar Foundation, Doha, Qatar
[b] College of Science and Engineering, Hamad bin Khalifa University (HBKU), Qatar Foundation, Doha, Qatar

ARTICLE INFO

Article history:
Received 30 April 2015
Accepted 2 September 2015
Available online 16 October 2015

Keywords:
Photovoltaics (PV)
Evolutionary algorithms
PV cell electrical parameters extraction
Temperature effects
Particle swarm optimization (PSO)
Cuckoo search (CS)

ABSTRACT

Photovoltaic (PV) cells induce current–voltage (*I–V*) characteristics dependent on the PV cell technology, the thin film structure and their eventual flaws during the elaboration process. The operation conditions also have a relevant impact on electrical curves characterizing these devices. The electrical parameters can be extracted from a PV panel standard datasheet using the commonly encountered single and double diode equivalent models representing the PV cell. This was done, in the present paper, at the most fundamental expression of these two models using evolutionary algorithms implemented in MATLAB (i.e. metaheuristic optimization methods). Four different *I–V* characteristics were available for the investigated commercial PV panel. They were fitted separately using the diode models and then taken as a whole to obtain parameters as physically meaningful as possible for the whole temperature range. The metaheuristic methods performed well for this problem, especially the cuckoo search algorithm. However, even with a good fitting of the fundamental behavior of the *I–V* characteristics, the presented approach may yield optimized solutions not as physically correct as it was expected. Thus, care must be taken for correctly interpreting the optimization results.

1. Introduction

Nowadays, photovoltaic (PV) conversion devices are major players in industrialized countries towards the production of more sustainable energy in their energy mix, also with possible applications outside the frame of conventional electrical grids. Within the so-called green economy, projects for PV plants/farms, or the integration of PV panels into buildings, all have a budget that is sensitive to the electricity output prediction over the life span of the PV devices. Numerous numerical models are applied to achieve such estimations by means of the PV panel's performance and its mounting geometry, thus making it possible to establish the PV module operating temperature as a function of service conditions simulation (see for example the model of King et al. [1] or of Sánchez Barroso et al. [2]).

Using these multi-physics models, the electrical power outputs are easy to quantify from the solar irradiance on the PV panels, assuming that the maximum electrical power is extracted from the PV device. Practically, it should be noted that this assumption is equivalent to a perfect operation of the maximum power point tracking device coupled to the PV inverter. From a theoretical point of view, establishing the maximum power point (P_{Max}) for a given model of a PV panel requires certain knowledge of the current–voltage (*I–V*) characteristic of this device. However, the *I–V* curve of a given PV panel/module/cell greatly depends on its temperature, real light irradiance, and is also a function of the PV cell technology. PV cells, as the core of this photoconversion process, are indeed manufactured as multilayered thin films of semiconductors with complex electronic features and dependence to the service conditions.

The approach proposed in this paper relies on the extraction of the intrinsic parameters which accurately describe the experimental *I–V* curves through the formalism of semi-empirical functions of these parameters (these semi-empirical functions apply well to the PV devices in general). Fundamentally, these semi-empirical relations consider the PV cell as an equivalent electrical circuit that can be the single-/one-diode model illustrated in Fig. 1 or the double-/two-diode model represented in Fig. 2 (see for instance [3,4]). These two equivalent circuits are well-established concepts that have been used for decades to extract the parameters of the illuminated PV cell *I–V* characteristics. In the 1980s, for example, a Newton–Raphson method was presented to resolve deterministically the one- and two-diode models of different PV cells [5]. Fitting techniques were exploited 10 years earlier on silicon solar cells [6] (even for the two-diode model). Our approach aims at finding good solutions using metaheuristic methods (implying stochastic schemes) for the same systems of semi-

* Corresponding author.
E-mail addresses: nbarth@qf.org.qa (N. Barth), sahzi@qf.org.qa (S. Ahzi).

http://dx.doi.org/10.1016/j.solmat.2015.09.003
0927-0248/

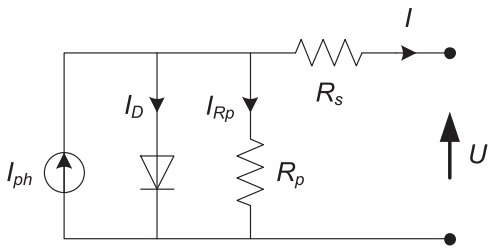

Fig. 1. One-diode equivalent circuit.

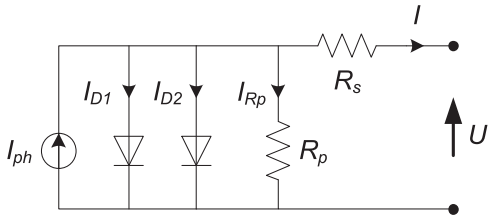

Fig. 2. Two-diode equivalent circuit.

empirical relations. This method can be applied to any kind PV cell. Similar techniques, based on evolutionary algorithms, have been widely applied to problems in the field with great success [7–17].

It should be noted that the parameters, used to describe the system, are physically based within their well-established context, using relations of the literature that are described in Section 2. Because of this fact, the optimization methods will only explore parameter values that are physically viable. To be exact, we will explore domains for each of them that are equivalent to the ones used in literature, at least in the order of magnitude.

In general, experimental *I–V* curves are characterized using common electrical equipments for different fixed temperatures and irradiance conditions [3]. For instance, these conditions can be defined by the conventional "standard test conditions" (STC) which imply that the PV cell receives 1000 W/m^2 of solar irradiance at 25 °C (the light spectrum being of an optical air mass at AM1.5). In a PV panel datasheet, provided by the manufacturer, details on the *I–V* characteristics are easily found at STC but also at other test conditions with other temperatures. We rely here on these kinds of data. We may use many experimental data, but we need at least three sufficiently different points on each *I–V* characteristic for fitting purpose. This requirement is easy to achieve since the datasheet generally contains reports of the maximum electrical power point P_{Max} and of the extreme values of the *I–V* characteristic under solar irradiance (namely, they are I_{SC} the short circuit (SC) current of the device and V_{OC} its open circuit (OC) potential/voltage).

Methods with different optimization (i.e. fitting) schemes and with physically-based parameters settings (e.g. from measurements) are commonly used in the literature to approximate the *I–V* characteristics. At their core, they are expressed with more or less unknown values of key parameters at the given reference temperature T_{Ref}, e. g. $T_{Ref} = 25$ °C for the STC, as in the case of the method based on the 5-parameter model proposed by De Soto et al. [18]. The aim of these methods is to use known data, generally provided by the manufacturer, to extrapolate the electrical performance of the PV devices to other atmospheric conditions than the STC. The point of these methods is to make it possible to simulate the electrical behavior in real service conditions. In their work, De Soto et al. [18] have shown that, for several types of PV technologies, the extrapolations can be done using common semi-empirical relations.

The semi-empirical expressions lying behind this field (of the extraction of electrical parameters relative to the PV technologies) are not particularly in focus here by themselves, but the literature is abundant on the subject. New developments or emergence of different expressions are also possible within the field, see for instance the recent improvement proposition related to the temperature and irradiance relation in Ref. [19], or another proposition to consider R_s in the one-diode model proportional to the current with $R_s(I) = R_{s0}(1 + K \times I)$ [17]. Taking this concern into consideration, it should be noted nevertheless that the proposed approach does not critically depend on eventual modifications made to the semi-empirical relations used explicitly in Section 2.

Here, we will use in the same fundamentals as the aforementioned semi-empirical approaches, but as much as possible with less relations correlating the parameters (or parameters anchored to physical measurements). Instead, we only rely on the optimization techniques to search for the fundamental physically based parameters.

At first, we apply this approach to the isothermal *I–V* characteristic data given at different T_{Ref} using only a PV panel datasheet. On the other hand, we want to take into account the temperature dependence of these parameters with more refined semi-empirical relations and parameters. This is still achievable within the framework of optimization techniques by considering the data set of the different isothermal conditions as a whole anisothermal set. It should be noted that the same approach could also be applied to solar irradiance variations (which are outside the scope of this paper). Both approaches were for example undertaken by Ma et al. [11] using the single diode model.

The proposed approach takes then into account the temperature effects. By doing so we can extrapolate judiciously to totally different atmospheric conditions in comparison to the STC. This can be done without favoring the accuracy of only one type of atmospheric conditions among low, STC, mid-high or higher temperature conditions. This is particularly pertinent for countries like Qatar, since summer temperatures and solar irradiance induce a PV cell temperature up to around 70 °C. In this study, we are less focused on very low temperatures or aerospace conditions but the proposed approach would remain valid.

2. Electrical modeling of PV panels

PV panels are modular devices assembled by connecting the solar cells in series and parallel following the design chosen by the manufacturer. We mentioned above the single or double diode equivalent circuits, but these models are applied mostly at the PV cell level. In our study, we focus however on using the data from a solar panel (BP 350 U [20]), which is comprised of two strings of PV cells connected in parallel. Each string for this particular panel has 36 PV cells connected in series. The PV cell *I–V* characteristic can then be directly taken from the panel's experimental *I–V* curves by dividing the current *I* by 2, the number of parallel strings, and by dividing the potential *U* by 36, the number of PV cells in series in each string [4]. The experimental *I–V* curves are available in the datasheet at four different temperatures. There exist also an alternative to using such experimental data for testing/validating purposes of these kinds of approaches, for instance see Ye et al. [7] with their use of synthetic data points elaborated for frankly different cases of *I–V* curves.

Regarding the equivalence used in the framework of the one- and two-diode models, we assumed here that the electrical parameters are relative to the concerned PV cell's total surface area, but it should be noted that the correct generalized values would be in terms of currents as Ampere per unit area (A/$\mathcal{A}$), and for the electrical resistances units of Ω× unit area $\mathcal{A}$. The scope of this paper is to present an optimization method to be applied to solar cells samples, solar cells, PV modules/panels/arrays, so this approach is unconcerned here with the changes in unit or formalism over the physical grounds of these equivalent circuits.

In the equivalent one- and two-diode circuits, illustrated in Figs. 1 and 2, I_{ph} is the photocurrent intensity generated by the illumination of the solar cell (with a direct proportional relation between illumination and current), $I_{D(1\text{ or }2)}$ is/are the dark current passing through the diode(s). R_s is the common series resistor (in series on the current generator) and R_p is the common parallel resistor also known as "shunt resistance". Finally, I is the current of interest going out of the equivalent electrical model and representing the current of the PV cell, and U its electric potential or voltage. The resistors have physical meaning [3], and it can be noticed that without them we would have $I_{ph}=I_{SC}$ the short circuit current (by convention, I–V plots are here in the first quadrant).

2.1. One-diode model

The single diode circuit of Fig. 1 implies [4,3,21]:

$$I = I_{ph} - I_0 \times \left[\exp\left(\frac{q(U+I\times R_s)}{A\times k_B\times T}\right)-1\right] - \frac{U+I\times R_s}{R_p} \tag{1}$$

where I_0 is the diode saturation current, A the diode ideality factor, q the elementary charge, k_B the Boltzmann constant, and T the temperature in K.

Values are usually around $[\mathcal{A}\cdot]R_s = 0.5\times10^{-4}$–$2\times10^{-4}\ \Omega\,m^2$ and $[\mathcal{A}\cdot]R_p = 0.2$–$2\ \Omega\,m^2$ [4]. $[\mathcal{A}\cdot]R_p$ for mass produced crystalline silicon cells is also reported to be several times $0.01\ \Omega\,m^2$ [3].

As for the dark current characteristic, the diode ideality factor A is typically 2 with a saturation current of $I_0[/\mathcal{A}] = 10^{-5}$–$10^{-4}$ A/m^2 at 300 K for silicon at low currents, and A is typically 1 for silicon at high currents [21].

2.2. Two-diode model

The double diode model relies on two diodes to model the dark current instead of only one (originally, I_D of the one-diode model). The two diodes have the same thermal voltage k_BT/q but with different ideality factors and saturation currents. Following the circuit presented in Fig. 2, the current–voltage characteristic becomes

$$I = I_{ph} - I_{0;1}\times\left[\exp\left(\frac{q(U+I\times R_s)}{A_1\times k_B\times T}\right)-1\right] - \frac{U+I\times R_s}{R_p} - I_{0;2} \times\left[\exp\left(\frac{q(U+I\times R_s)}{A_2\times k_B\times T}\right)-1\right] \tag{2}$$

where $I_{0;i}$ and A_i are the new diode saturation currents and ideality factors associated with the two dark currents I_{Di}.

Ideal values for the diodes are $A_1=1$ and $A_2=2$, and industrial samples having 16% efficiency were reported with the estimation of $1\le A_1\le 1.5$ and $2\le A_2\le 5$ [17]. Moreover, it can be raised from the literature that many authors assume the ideal case $A_1=1$ and $A_2=2$ when they are considering the two-diode model.

2.3. Subsequent thermal dependence of the parameters

The electrical parameters characterized in PV cells can be found to be thermal dependent in the literature through different complementary (semi-)empirical relations. We expect that these detailed relations will enable us to project the different experimental isothermal I–V characteristics into an anisothermal parameter space.

Other scarce cases in the literature deal with truly anisothermal I–V characteristic points (which are outside the scope of the current study). The experimental points used there to extract electrical parameters are actually including evolving temperature within them. For example, this can be done if they are taken from a parametric window of atmospheric conditions [10].

2.3.1. Diode saturation current I_0

The thermal dependence of the diode saturation current follows an Arrhenius law with the following Boltzmann factor [3]:

$$I_{0;i}(T) = I_{00;i}\times\exp\left(-\frac{E_A}{k_B\times T}\right) \tag{3}$$

with "; i" being blank, "; 1" or "; 2" depending respectively on the one- or two-diode models and the diode that is concerned; E_A is the thermal activation energy that we chose common for both diodes in the two-diode model. For crystalline silicon solar cells it should be around 1.1 eV. The temperature-independent pre-factor $I_{00;i}[/\mathcal{A}]$ can be rather high, e.g. 10^6 A/m^2.

Another relation found in the literature, for example described by Tsai [22] for a single diode equivalence, is the following and depends on the band gap E_G and the ideality factor which are also fluctuating with the temperature (see for example Refs. [11,12,18] for further details and neighboring relations):

$$\frac{I_0(T)}{I_{0;Ref}} = \left(\frac{T}{T_{Ref}}\right)^3\times\exp\left[\frac{q\times E_G(T)}{k_B\times A(T)}\left(\frac{1}{T_{Ref}}-\frac{1}{T}\right)\right] \tag{4}$$

where $I_{0;Ref}$ is the diode reverse saturation current at the reference temperature T_{Ref}.

2.3.2. Diode ideality factor A

The ideality factor for the diodes is also temperature-dependent [3] and is given through the following power form for example, derived from Ref. [23]:

$$A_N(T) = A_{0,Ref;i}\left(\frac{T}{T_{Ref}}\right)^{a^{(i)}} \tag{5}$$

with $A_{0,Ref;i}$ the pre-factor and $a^{(i)}$ the power exponent. T_{Ref} was chosen at the mean value of all the temperatures here, i.e. approximately 311 K.

2.3.3. Photocurrent I_{ph}

The photocurrent varies with the following temperature- and irradiance-dependent form [23]:

$$I_{ph} = \left(\frac{S}{S_{Ref}}\right)^m\left[I_{ph,Ref}+\mu_{I_{SC}}(T-T_{Ref})\right] \tag{6}$$

About Eq. (6), we note that we do not consider other solar irradiance conditions than STC, so the total absorbed irradiance S equals S_{Ref} and the coefficient m will not be used. We also note that $I_{ph,Ref}=I_{ph}(25\ ^\circ\text{C})$ is still to be determined within the sets of parameters, and that we can then shift linearly this parameter to the other needed temperatures by using the coefficient $\mu_{I_{SC}}$. The same translation of this parameter can be applied after the relations given by De Soto et al. [18] or by Ma et al. [11], since they proposed very similar expressions containing optical modifier factors that also have no point in our current applications.

2.3.4. Resistors R_s, R_p

For the series resistor R_s, the temperature dependence can be described as a positive temperature coefficient type [24]:

$$R_s(T) = R_{s0}\times\exp(B_s\times T) \tag{7}$$

where R_{s0} is the condition resistance and B_s is the semiconductor material coefficient with $B_s>0$. For the shunt resistor R_p, the temperature dependence can be described in the negative temperature coefficient form [25]:

$$R_p(T) = R_{p0}\times\exp\left(\frac{B_p}{T}\right) \tag{8}$$

where R_{p0} is the initial condition resistance and B_p is the semiconductor material coefficient with $B_p>0$.

3. Evolutionary algorithms

We obtained from the four experimental isothermal *I–V* curves two kinds of data points relevant to the optimization techniques: on the one hand, $data_T^{optim}$ that are several spaced points on the isothermal curves to use as objective points for the evolutionary algorithms (11 points per isothermal *I–V* curve). On the other hand, we obtained also the $data_T^{check}$, which are multiple points digitized from the experimental *I–V* curves to check the results of the evolutionary algorithms. For details, refer to Online Resource 1, and see also the spreadsheets containing all of these points that are available in Online Resource 2.

It should be noted that for the datasheet of BP 350 U, where the value of $\mu_{I_{SC}}$ was given at $0.065 \pm 0.015\%/°C$, we chose a better estimation at 0.08%/°C, i.e. ≈ 2.54 mA/°C at the electrical level of the PV panel. This was done because the data curves did not seem coherent with the mean value taken as is. In the current optimization approach, this value is transformed into a parameter belonging to the search space in order to be even more accurate for this crucial effect (the optimization points were however kept at the value of 0.08%/°C).

The evolutionary algorithms are managing a population of N_{pop} individuals represented by points in a *n*-dimensional search space, where *n* is the number of parameters to fit the experimental data. Each individual is a candidate for the optimization of the *n* parameters. In practice, the optimization scheme uses evolutionary means to draw individuals nearer to an idealized zero difference between the modeled curve and the experimental results used for fitting purposes. This requires an objective function to compare the individual between them at each increment of these methods. Then, each individual can be ranked by this function returning a scalar value. In evolutionary algorithms, the objective function is also called the fitness function, since the evolutionary process relies on selection processes similarly to the mechanisms of Nature, e.g. the survival of the fittest, etc.

The fitness function X_{fit} is a norm set from an individual to the number of experimental points (used to optimize these parameters/individuals). If the method is successful, the best individual converge after numerous increments towards the minimum norm possible (global minimum). Within reasonable computation times, these kinds of optimization techniques allow us to browse vast search spaces and find good fitting solutions (i.e. global or good local minimums). Finding of the mathematical optimal solution with these techniques is in general only guaranteed for infinite computation time. Due to the non-linearity, resulting from the model definition, of fitness function X_{fit} given in Eq. (9), and its dependence on multiple parameters, it was necessary for some of the methods applied to use a meta-heuristic approach for minimization (e.g. coupling the global exploration to a more efficient local exploitation algorithm that is deterministic).

In this section, we will first describe the evaluation of the proposed models for single and two-diode systems given in Eqs. (1) and (2). Afterwards, we will describe the evolutionary algorithms and/or their parameters we selected to deal with the extraction of the *I–V* characteristic parameters for PV cells. After a short review on similar problems in the field of the PV diode models, the following algorithms have been applied: particle swarm optimization (PSO) [7,9–12,14–17] and genetic algorithm (GA) [7–9,11–14]. In this work, we also explore the suitability of the recent optimization method "cuckoo search" (CS) for the problem of interest, which was also undertaken for a one-diode model in Ref. [11].

In a former study, the CS method was also applied within the PV field. Instead of the current approach on the extraction of electrical parameters of the PV cells, it was used for optimization problems regarding the optical sizing via the electronic properties of multi-junctions and split spectrum solar cells [26].

Some of the aforementioned studies [12,14] also contained hybridized metaheuristic approach to research more efficient ways of optimization. We did the same for CS. To be exact, the original CS algorithm and its hybridization with the Nelder–Mead Simplex method (CS-NMS) [26] have been compared to the frequently used GA and PSO. The CS-NMS has been included due to the fact that it has been designed to find solutions for problems with a small number of parameters (2–10) and with a low number of evaluated fitness functions, while the original CS is a general optimization method.

Both of the diode models have been evaluated for the 4 available temperatures of 0 °C , 25 °C, 50 °C and 75 °C. The computational experiments have been performed for each and also for all of the temperatures at the same time. In practice, this means that there were 10 test functions (8 with the $\Theta_T^{(i)}$ introduced below in Eqs. (13) and (15), and 2 for each $\Xi^{(i)}$ introduced in Eqs. (17) and (19)). With the goal of having an extensive comparison of the methods, 20 separate runs have been performed for each of the algorithms on the different test functions. The stopping criterion for each of the methods was that 10,000 fitness functions have been evaluated for the 5-parameter single diode problem that will be introduced below, and 20,000 fitness functions for all the other models.

The computational experiments have been coded using MATLAB (v. R2013b, MathWorks ®) to implement the evolutionary algorithms. The tests for the CS algorithm have been performed using the code developed by Yang [27]. For the CS-NMS, we have used the MATLAB code provided by the authors, which is available online [28].

3.1. General principles and model evaluation

For any given set "*E*" of N_E experimental data points to fit, the initialization of N_{pop} individuals is done by scattering them randomly over the *n*-dimensional search space. We note Θ their coordinates (equals the *n* parameters) and $X_{fit}(\Theta, E)$ their fitness function. N_E being the size of *E*, the generic *k*th point to fit on the experimental *I–V* curve plane is noted $[E_k^I, E_k^U]$. Moreover, for the $data_T^{optim}$ introduced in the Online Resource 1, we chose the first experimental point as defined by $I_{SC}(T) = (E_1^I, 0)$ and the last one by $V_{OC}(T) = (0, E_{N_E}^V)$. In our optimization scheme, 9 other points are digitized in between from the experimental curve ($N_E = 11$ for each temperature).

The parameters of the diode models are hereafter optimized for a minimal value of the following chosen fitness functions:

$$X_{fit}(\Theta, E) = \sum_{i=1}^{N_E} |E_k^I - I_{calc,k}| \frac{1}{N_E} \tag{9}$$

For the PV cell parameters extraction field, Siddiqui and coworkers used the following normalized error expression, using $E = \{I_{SC}, P_{Max}, V_{OC}\}$ which covers three meaningful points generally easy to get from the PV panel datasheets [12,29]:

$$J_{fit}(\Theta, E) = \left|\frac{I_{P_{Max},calc} - I_{P_{Max},\exp}}{I_{P_{Max},\exp}}\right| + \left|\frac{U_{P_{Max},calc} - U_{P_{Max},exp}}{U_{P_{Max},exp}}\right| + \left|\frac{I_{SC,calc} - I_{SC,exp}}{I_{SC,exp}}\right| + \left|\frac{U_{OC,calc} - U_{OC,exp}}{U_{OC,exp}}\right| + |I_{OC}| + \left|\frac{dP(P_{Max})}{dV}\right| \tag{10}$$

Ye et al. [7] used an objective function based on the root mean square error over the $[E_k^I, E_k^U]$ points:

$$K_{fit}(\Theta, E) = \sqrt{\frac{1}{N}\sum_{k=1}^{N} y^2\left(E_k^I, E_k^U, \Theta\right)} \tag{11}$$

where

$$y\left(E_k^I, E_k^U, \Theta\right) = \begin{cases} I - I_{ph} + I_D + I_{R_p} & \text{(one - diode model)} \\ I - I_{ph} + I_{D1} + I_{D2} + I_{R_p} & \text{(two - diode model)} \end{cases} \quad (12)$$

Except analytical approaches on the one- or two-diode models, i.e. parametric Eqs. (1) or (2), very few authors detail how they solve the parametric equation between U and I implemented within their fitness function under such statements as "the model parameters Θ are to be applied to an experimental point", or Eq. (12). Other authors use the formalism of Lambert W function for the studies undertaken in the field [14,30], but the complete mathematical modeling (out of the scope of this paper) is overlooked here.

For the current approach, we resolved this numerically by (i) fixing the potential in the parametric curves to the electrical experimental value E_k^U; (ii) making I vary over a "I-range" within values in an interval from ≈ -1 A to ≈ 1 A above the maximum of the experimental current values for the whole data sets. (iii) The minimum difference obtained for a "I-resolution" of 10^{-2} A on the I-range is then assumed to verify Eqs. (1) or (2) and this value of I on this mesh is the approximated value of I_{calc} adequate for the fitness function $X_{fit}(\Theta, E)$, meaning that this I_{calc} is then compared to the experimental currents E_k^I.

This simple (but costly) numerical method was chosen to avoid relying too much on higher level mathematical solvers or functions, thus allowing easy transpositions of the algorithms to any language. In a former work using PSO method for example [15] (re-conducted also here), we used a better resolution by two orders of magnitude but with 4 times less experimental points. If the accuracy of the fitness function is needed, the I-resolution should be at least of 10^{-4} A.

Finally, we also investigate better estimates of the fitness function with the data used to verify the proposed solution (with $data_T^{check}$ points). We did only this at the end of the optimization scheme (as overexploitation was not investigated). The computational cost of the fitness function is then irrelevant and we refined the I-resolution by three orders of magnitude compared to the one used in the optimization scheme. I-range was also reduced to $[-0.05;\ 1.75]$ A at the PV cell level.

With these assumptions, we aim in this approach at keeping a good precision of the modeled curve by taking numerous and varied $data_T^{optim}$ points from the experimental I–V characteristics. With the current fitness function, we also note that the I–V candidates are optimized during the process with a more rigorous criterion regarding their V_{oc} branch (through both more points on this branch, and by the kind of mathematical norm we apply). This is appropriate here, since we want to evaluate the temperature effects which are more important on the V_{oc} branch. We did not undertake in this study a sensitivity analysis of the method depending on where the optimization points are more concentrated, e.g. towards the maximum power point or the branches.

3.1.1. Isothermal optimums, parameters and search space

Using Eq. (1) for the single diode model at different fixed isothermal conditions, the set of 5 parameters to be found using evolutionary algorithms is listed in the following order:

$$\Theta_T^{(1)} = \{I_{ph}, I_0, A, R_s, R_p\} \quad (13)$$

for which the following search space is chosen:

$$\{[1;2]\,\text{A}, [0;10^{-4}]\,\text{A}, [0.5;2.5], [0;2]\,\Omega, [50;10^4]\,\Omega\} \quad (14)$$

Using Eq. (2) for the double diode model, the set becomes one of 7 parameters:

$$\Theta_T^{(2)} = \{I_{ph}, I_{0;1}, A_1, I_{0;2}, A_2, R_s, R_p\} \quad (15)$$

for which the search space is extended to:

$$\left\{[1;2]\,\text{A}, \left[0;10^{-4}\right]\,\text{A}, [0.5;1.5], \left[0;10^{-4}\right]\,\text{A}, [1.5;3.5], [0;2]\,\Omega, \left[50;10^4\right]\Omega\right\} \quad (16)$$

As a case study, we reduced also $\Theta_T^{(1)}$ to a much smaller set in the framework of a previous study [15] concerning the PSO method applied to the single diode model at STC. In this study, the reduction of parameters originally relied on other kinds of well-established relations for the photocurrent I_{ph}, for the diode reverse saturation current I_0 and for the ideality factor A. The details of the used relations are explicitly listed in Appendix A. The remaining search space is defined then by only two parameters $\{R_s, R_p\}$ that we adapted in the current case study over $\{[0;2]\,\Omega, [0;10^4]\,\Omega\}$. We conduct again this exploratory study inside the Online Resource 1 with the present formalism. However, we still used the same original three points of the I–V characteristic (instead of $E = \text{data}_{25°C}^{optim}$, we have here $E = \{I_{SC}, P_{Max}, V_{OC}\}$).[1]

In other publications concerning similar methods, the search space is scarcely mentioned. Either way, we can rely on the physical grounding of the parameters and their expected range. In the literature concerning $\Theta_T^{(1)}$, we note that Ye et al. [7] searched within the following space for their experimental parameters extraction study: $\{[1;2]\,\text{A}, [0;10^{-4}]\text{A}, [0;3.5], [0;0.05]\Omega, [0;250]\Omega\}$. As for their two-diode application with $\Theta_T^{(2)}$, the same authors searched within the space: $\{[1;2]\,\text{A}, [0;10^{-4}]\,\text{A}, [0;3.5], [0;5\times10^{-8}]\,\text{A}, [0;2], [0;0.05]\,\Omega, [0;250]\,\Omega\}$.

3.1.2. Unique set of multi-T parameters

For anisothermal conditions, the relations chosen to describe the thermal behavior of all the available I–V curves optimized at the same time are Eq. (3), and Eqs. (5) to (8).

Adding to these relations Eq. (1) for the single diode model, we obtain a 10-parameter set to be found, listed by

$$\Xi^{(1)} = \{I_{ph,Ref}, \mu_{I_{SC}}, E_A, I_{00}, A_{0,Ref}, a, R_{s0}, B_s, R_{p0}, B_p\} \quad (17)$$

for which the search space is chosen to be

$$\{[1;2]\text{A}, [1\times10^{-3};1.5\times10^{-3}]\,\text{A}/°\text{C}, [0.5;1.3]\,\text{eV}, [0;10^{11}]\,\text{A}, [0.5;5]\text{ at }311\text{ K}, [0.4;1.5], [0;1]\,\Omega, [0;0.1]\,\text{K}^{-1}, [50;10^4]\,\Omega, [5;11]\times10^2\,\text{K}\} \quad (18)$$

Adding instead Eq. (2) for the double diode model, the set becomes one of 13 parameters listed by

$$\Xi^{(2)} = \{I_{ph,Ref}, \mu_{I_{SC}}, E_A, I_{00;1}, A_{0,Ref;1}, a^{(1)}, I_{00;2}, A_{0,Ref;2}, a^{(2)}, R_{s0}, B_s, R_{p0}, B_p\} \quad (19)$$

for which the search space is chosen to be

$$\{[1;2]\,\text{A}, [1\times10^{-3};1.5\times10^{-3}]\,\text{A}/°\text{C}, [0.5;1.3]\,\text{eV}, [0;10^{11}]\,\text{A}, [0.5;5]\text{ at }311\text{ K}, [0.4;1.5], [0;10^9]\,\text{A}, [2.5;7]\text{ at }311\text{ K}, [0.4;1.5], [0;1]\,\Omega, [0;0.1]\,\text{K}^{-1}, [50;10^4]\,\Omega, [5;11]\times10^2\,\text{K}\} \quad (20)$$

It can be noted that in these $I_{ph,\ Ref}$ could be at any temperature within the ones reported in the datasheet, given the fact that its range is sufficiently large to permit all the values foreseen, linked to $I_{SC}(0\ °\text{C})$ up to $I_{SC}(75\ °\text{C})$.

[1] It can be noted, for the short case study only, that we used the J_{fit} fitness function containing also the derivative at P_{Max} (see Eq. (A.4). Other noteworthy implementation details are that initial speeds were chosen at random numbers between 0 and 1. Finally, we corrected in the current work the value of $\max(R_p)$ of the search space for $\{R_s, R_p\}$. In the initial study, the search space was indeed too reduced, being $\{[0;2/36]\,\Omega, [0;300/36]\,\Omega\}$. It is now $\{[0;2]\,\Omega, [0;10^4]\,\Omega\}$. The number of J_{fit} functions evaluated is for this initial protocol 50,000 for 50 individuals.

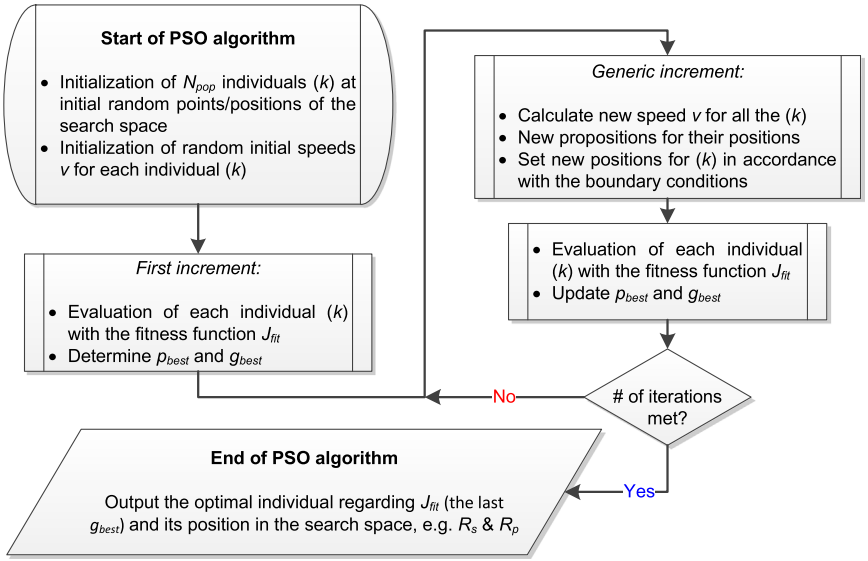

Fig. 3. Flowchart for the PSO method [15].

All the parameter values and physical grounding described earlier in Section 3.1.1, about the isothermal cases, should prevail here in the non-isothermal cases.

Concerning the set of parameters $\Xi^{(1)}$, a PSO method was implemented [10] with real-time data points encompassing non-constant temperatures. Simplifications were applied to $\{I_{ph}, I_0\}$ in order to reduce these parameters to fixed expressions, eventually through measurements, thus leading to a 3-parameter/dimensional search. In the PSO method they propose, $\{A, R_s, R_p\}$ were searched within the following search space: $\{[0;2],[0;20]\,\Omega, [10;200]\,\Omega\}$.

3.2. Selected evolutionary algorithms and implementation

3.2.1. PSO method

The particle swarm optimization (PSO) belongs to the nature-inspired optimization techniques and is able to solve the problems undertaken in this PV field [15]. The PSO algorithm is described by Eberhart and Shi [31]. For a total of N_{iter} iterations and for each individual (k), its main equations are given by Eqs. (21) and (22), following the flowchart in Fig. 3.

In the present PSO method, with X_{fit} fitness function, the current parameters were chosen to be identical to some of the conditions already tested in Ref. [15] but favoring the exploration. N_{pop} is 50 for the 5-parameter model, and 200 for the other models. As it was done in this former study, we do not take into account the size of the time steps in the following velocity definition, and it can also be noted that the initialization of the speeds were chosen at a random number between 0 and 1 ($=rand()$) times 25% of the search space range for each parameter:

$$v_n^{(k)} = i_w \times v_{n-1}^{(k)} + rand() \times c_1 \left(p_{best;n-1}^{(k)} - x_{n-1}^{(k)}\right) + rand() \times c_2 \left(g_{best;n-1}^{(all)} - x_{n-1}^{(k)}\right) \quad (21)$$

with i_w the inertia for the particles, chosen to be 0.4 in the current applications. c_1 and c_2 are parameters that direct the convergence of the population towards the best particle parameters ($g_{best}^{(all)}$) and also taking into account the local exploitation with the position of each (k) particle at the best of their fitness ($p_{best}^{(k)}$). We chose $c_1 = 2$ and $c_2 = 1$. This velocity is then used to update the position:

$$x_n^{(k)} = x_{n-1}^{(k)} + v_n^{(k)} \quad (22)$$

using reflective boundary conditions at the limit of the search space.

The above-mentioned parameters and N_{pop}, and the number of applied test functions, are not especially optimized to deal with the current applications of the PSO algorithm (all of these could be finely tuned to this particular problem, but this is out of the scope of the study). All the detailed results of the PSO algorithm are given in Online Resource 2.

3.2.2. CS and CS-NMS

Cuckoo search (CS) [32,33] is a novel optimization method that has proven its effectiveness on a wide range of problems [34]. In the recent years, it has gained significant popularity due to its simplicity and robustness. It has been successfully applied to many engineering problems [35]. As already stated, the original CS algorithm has been also hybridized with the Nelder–Mead Simplex method (CS-NMS) [26].

For the sake of completeness we include a short outline of the original CS algorithm introduced by Yang [32]. This metaheuristic is inspired by the behavior of some cuckoo species. Cuckoos do not make nests but hide their eggs in ones belonging to other host birds (of other species). The evolutionary process has made it possible for cuckoos to mimic the shape and color of some specific hosts. This mimicry is a result of the fact that if a host bird discovers the intruder eggs are not their own, it will either throw these eggs or simply abandon its nest and build a new one at a new location. If the cuckoo eggs manage to hatch, the cycle is repeated.

This concept has been converted into a population based metaheuristic in the following way. Each egg in a nest will be considered as a solution, and the cuckoo eggs will correspond to the newly generated solutions which will be highly similar to the original one in the nest. This is done in the hope that such solutions will potentially be better. The new solutions will be used to replace the lower quality nests (solutions). In the simplest form, each nest contains only a single solution. The CS algorithm uses the following three idealized rules:

1. Each cuckoo in the colony randomly selects one nest and creates a single egg (solution) which is similar to the one that corresponds to the nest.
2. The best solution will be carried to the next generation.
3. The number of available hosts nests is fixed, and the egg laid by a cuckoo is discovered by the host bird with a probability p_a. The

Table 1
Comparison of performance of PSO, GA, CS and CS-NMS algorithms applied to the single and two-diode models for the experimental data. These values of $X_{fit}(data_T^{optim})$ are given here as the minimal, average and standard error for each 20-run series, in $\times 10^{-2}$ A per data point. The unique best values are underlined (i.e. best minimum values and best average, underlining so the efficient methods).

Temperature(°C)	PSO		GA		CS		CS-NMS	
	Min	Avg(Std)	Min	Avg(Std)	Min	Avg(Std)	Min	Avg(Std)
One-diode (5 parameters, i.e. for each T and for all of the 20-run series of $\Theta_T^{(1)}$)								
0	3.8	17.4(27.4)	2.4	4.9(1.6)	2.7	3.4(0.6)	1.8	4.5(1.4)
25	1.7	8.9(5.7)	3.3	7.8(6.5)	2.3	3.0(0.7)	1.5	2.8(0.9)
50	2.9	9.7(9.1)	2.7	6.5(6.8)	2.5	3.7(0.3)	2.0	3.6(0.7)
75	0.8	8.3(8.4)	1.0	4.7(10.2)	0.8	1.3(0.2)	0.8	1.2(0.3)
Two-diode (7 parameters, i.e. for each T and for all of the 20-run series of $\Theta_T^{(2)}$)								
0	0.5	117.0(60.3)	0.5	22.6(29.7)	0.5	3.3(1.2)	0.5	13.9(26.4)
25	0.9	33.0(44.9)	0.9	5.0(7.8)	0.9	1.7(0.8)	0.9	5.0(13.3)
50	1.6	5.2(8.5)	1.2	2.6(1.4)	0.7	1.5(0.4)	1.4	2.0(0.3)
75	0.6	1.1(0.3)	0.8	1.3(1.0)	0.8	0.9(0.1)	0.6	1.0(0.2)

discovering (discarding) operation is only done on some set of worst nests.

Based on these rules we can explicitly define the CS algorithm using the following pseudocode:

1: Generate an initial population of N_{pop} host nests;
2: **while** ($t < MaxGeneration$) or ($stopcriterion$) **do**
3: Get a cuckoo randomly (say, i) and replace its solution by performing Levy flights;
4: Evaluate its quality/fitness F_i;
5: Choose a nest among N_{pop} (say, j) randomly;
6: **if** $F_i < F_j$ **then**
7: Replace j by the new solution;
8: **end if**
9: A fraction (p_a) of the worse nests are abandoned and new random ones are built;
10: Keep the best solutions/nests;
11: Rank the solutions/nests and find the current best;
12: Pass the current best solutions to the next generation;
13: **end while**

Levy flight is of essential importance for the CS algorithm. In practice, it generates a random walk which obeys a power-law step length distribution with a heavy tail. It has been shown that the use of Levy flight is much more effective in exploring the solution space than a simple random walk. We fixed $p_a = 25\%$.

The robustness of the CS algorithm lies in the sense that only one parameter, the number of nests, needs to be specified. The number of nests was 25, 20 for CS, CS-NMS respectively.

3.2.3. GA

The GA has been applied using the built-in MATLAB function. The parameters for it have been optimized by literature reference and empirical tests. The population size was set to 100, 200 out of which 2, 4 were considered as elitist for problems with 5, or more parameters, respectively. The crossover fraction was set to 0.8. The mutation was set by the MATLAB parameter value MUTATIONUNIFORM, which correspond to selection rate of 0.01.

4. Results and discussion

The result we present and discuss come from the 20 separate runs we have done for each of the algorithms and test functions related to the one- and double diode models, using the optimization points $data_T^{optim}$. The main isothermal cases are presented in Section 4.1 and the multi-T cases in Section 4.2. The exploratory study of Sánchez Barroso et al. [15] at STC, reducing the current approach to a minimalist problem in order to search for R_s and R_p, was undertaken as a preamble of the results of this section. This short case study can be found in Online Resource 1. The results presented here in the paper are all obtained over vaster dimensional spaces, and for much more experimental data points (all 44 of the $data_T^{optim}$ points) than the three points in the short case study ($E = \{I_{SC}, P_{Max}, V_{OC}\}$).

4.1. Optimization of the isothermal I–V curves

Results obtained for the iso-thermal I–V curves are given in this section (i.e. each temperature taken separately in the optimization/fitting scheme).

4.1.1. Global performance of the algorithms

To have a more exhaustive comparison of the methods, the best, average and standard deviation of the generated solutions, for each test function, are presented in Table 1.

The first conclusion that can be made from observing the results given in Table 1 is that the proposed models have a good correspondence to the experimental data. In case of the best fitted parameters, the error based on the measure given in Eq. (9) was between 0.8–2.0 cA per data point and 0.5–0.9 cA/point, depending on the temperature, respectively for the single and two-diode models. It is interesting to note that the error for the two-diode model was lower than for the single diode model. This indicates that the model is more suitable for the data, especially if we take into account that GA and CS generally have a weakened performance with an increase in the number of function parameters.

From the results given in Table 1, it is also evident that the two CS algorithms have a significantly more reliable performance than GA or PSO. To be exact, the average error for CS and CS-NMS is lower than the one of GA or PSO for all the tested functions. The performance of the two CS algorithms was dependent on the number of parameters that needed to be optimized. For functions with 5 parameters, CS-NMS acquired the best results, compared to the other methods, for both the minimal and average error in case of all the test functions. In case of 7 parameters, the original CS algorithm managed to have the lowest average error. The minimal error was similar for all the four methods, while being most consistent in case of CS. The advantage of the CS algorithm in case of the model with 7 parameters is not unexpected since the CS-NMS was designed to have the best performance for low dimensional problems when a low number of function evaluations is allowed.

Table 2
Best parameters found within each of the 20-run series for the single and double diode models, found by GA, CS and CS-NMS algorithms, see also Fig. 4 for the double diode models. It should be noted that the corresponding $X_{fit}\left(\Theta_T^{(i)}, data_T^{optim}\right)$ are the minimum values reported in Table 1. In the last column, the fitness function results are given for validity purposes for each $data_T^{check}$ set (values are in $\times 10^{-2}$ A per point, which is the same unit as with the $data_T^{optim}$ sets reported until now). Other units were given within the parameters' definitions in Section 3.1.1.

One-diode (5 parameters, i.e. $\Theta_T^{(1)}$)

T (°C)	I_{ph}	I_0	A			R_s	R_p	$X_{fit}(data_T^{check})$
0	1.554844	6.700408e−07	1.916272	.....	.....	6.111809e−03	5.041569e+03	2.5
25	1.585061	3.193259e−06	1.796817	.....	.....	5.047404e−03	5.226808e+03	2.9
50	1.623395	3.223374e−06	1.504602	.....	.....	1.080460e−02	1.719762e+03	2.8
75	1.653502	1.380656e−05	1.409675	.....	.....	9.099002e−03	9.222751e+03	2.6

Two-diode (7 parameters, i.e. $\Theta_T^{(2)}$). ‡ are values at the boundary of the search space

T (°C)	I_{ph}	$I_{0;1}$	A_1	$I_{0;1}$	A_2	R_s	R_p	$X_{fit}(data_T^{check})$
0	1.552101	5.362084e−09	1.446950	1.743092e−05	3.193308	1.420528e−02	3.640441e+03	1.0
25	1.579897	1.815445e−07	1.477021	1.723703e−05	3.201763	1.271318e−02	3.262464e+03	1.7
50	1.615102	1.541603e−07	1.221664	0 ‡	3.500000 ‡	1.818692e−02	1.982817e+03	1.2
75	1.653321	7.343167e−06	1.340359	6.672136e−05	2.471391	9.403295e−03	1.145731e+03	2.5

It is important to mention that in case of the GA, contrary to the other algorithms, a significant number of tests was necessary to fine tune the method parameters to be able to have a good performance.

4.1.2. Optimized 5- or 7-parameter diode models

We present in this section the best results out of the statistical analysis of the 20-run series of parameters undertaken for the four different isothermal *I–V* characteristics. The parameters with a minimum values of the X_{fit} fitness functions, i.e. optimized solutions, are given in Table 2. They are also illustrated in Fig. 4 for the two-diode model by superimposing these optimal results to the experimental data points $data_T^{optim}$ and $data_T^{check}$. Partial results from this approach, but with only one single run (among the 20 runs times the number of optimization techniques used), can be found in Online Resource 1.

One of the parameter sets from these partial results is found after the end of the optimization scheme with a series resistor having a 0 Ω value. We will discuss this particular result in Section 4.2.2.

Another interesting feature of the parameters reported within Online Resource 1, with the single runs only, is the fact that several of these optimal parameters have an ideality factor equals to zero in the double diode model. This means that the two-diode model has found a better set of parameters within the framework of the one-diode model (as the search space allows indeed in our approach the one-diode model to be included into the two-diode model). The extended domain search of the two-diode model does not impact much the best values of the fitness function found at the end of the optimization methods. This is also another reason why we found that the error for the two-diode model was lower than for the single diode model, adding to the fact that the two-diode model is apparently more adapted to the PV panels *I–V* characteristic data. This particular case of diode extinction is also happening for the 50 °C best parameter found even after 20 runs in Table 2.

4.2. Optimization over a unique set of multi-T parameters

In this final section, the optimization scheme is dealing with all of the $data_T^{optim}$ experimental points at the same time (the four different temperatures are equi-represented) and the parameters found can then be applied directly to any extrapolated temperature relevant to this whole data set.

4.2.1. Global performance of the algorithms

In Table 3, the performance of the proposed optimization methods were reported for the 10- and 13-parameter one- and two-diode models respectively. The maximum values for the fitness functions after the 20 runs were also added to the other types of performance statistics already introduced (i.e. minimum, average and standard deviation values; each run having its own stochastic minimum fitness function at the end of its optimization scheme). These results are coherent with the discussion about the global performance of the algorithms after Table 1. CS is still better than CS-NMS due to the fact that CS-NMS was designed for lower dimensionality. GA and PSO performed badly here, but we highlight the fact that they did not totally fail with these two more complicated functions here.

4.2.2. Optimized 10- or 13-parameter diode models

The best optimized solution from Table 3 for the 10-parameter one-diode model was reported in Table 4. We also reported there the best solution found by CS algorithms which performed better in general for the parameter extraction. In Table 5, we reported the best optimized solution from Table 3 for the 13-parameter double diode model. This optimum is also illustrated in Fig. 5. This latter optimum performed better than the one found for the single diode model after 20 runs (better performance with $data^{optim}$ and $data^{check}$), even if we are again in the case reported before with one of the diode current that is removed from the equivalent circuit by a factor at 0 A, thus reducing the two-diode model into the one-diode model. It can be noted that this better one-diode compatible parameter candidate was not found after 20 runs of the single diode model, however it is not known if this observation can be generalized for any number of runs undertaken for the optimization series (for instance, more runs for these series may help both diode models converge towards the same optimum).

Nevertheless, the two-diode model performs once again better than the one-diode model, even with more dimensionality. These optimums can drive at some increment of the optimization process the extinction of a diode within the two-diode model (and with our evenly repartitioned points on the *I–V* curves, which is perhaps also favoring by themselves a certain kind of dark current).

Moreover, it should be noted that a one-diode optimum reported in Table 4 presents also $R_{s0} = 0\ \Omega$, implying $R_s = 0\ \Omega$, which is the best result obtained after 20 runs for all temperatures as a whole. This was also happening in the partial results for isothermal cases, detailed in Online Resource 1, obtained after only single runs.

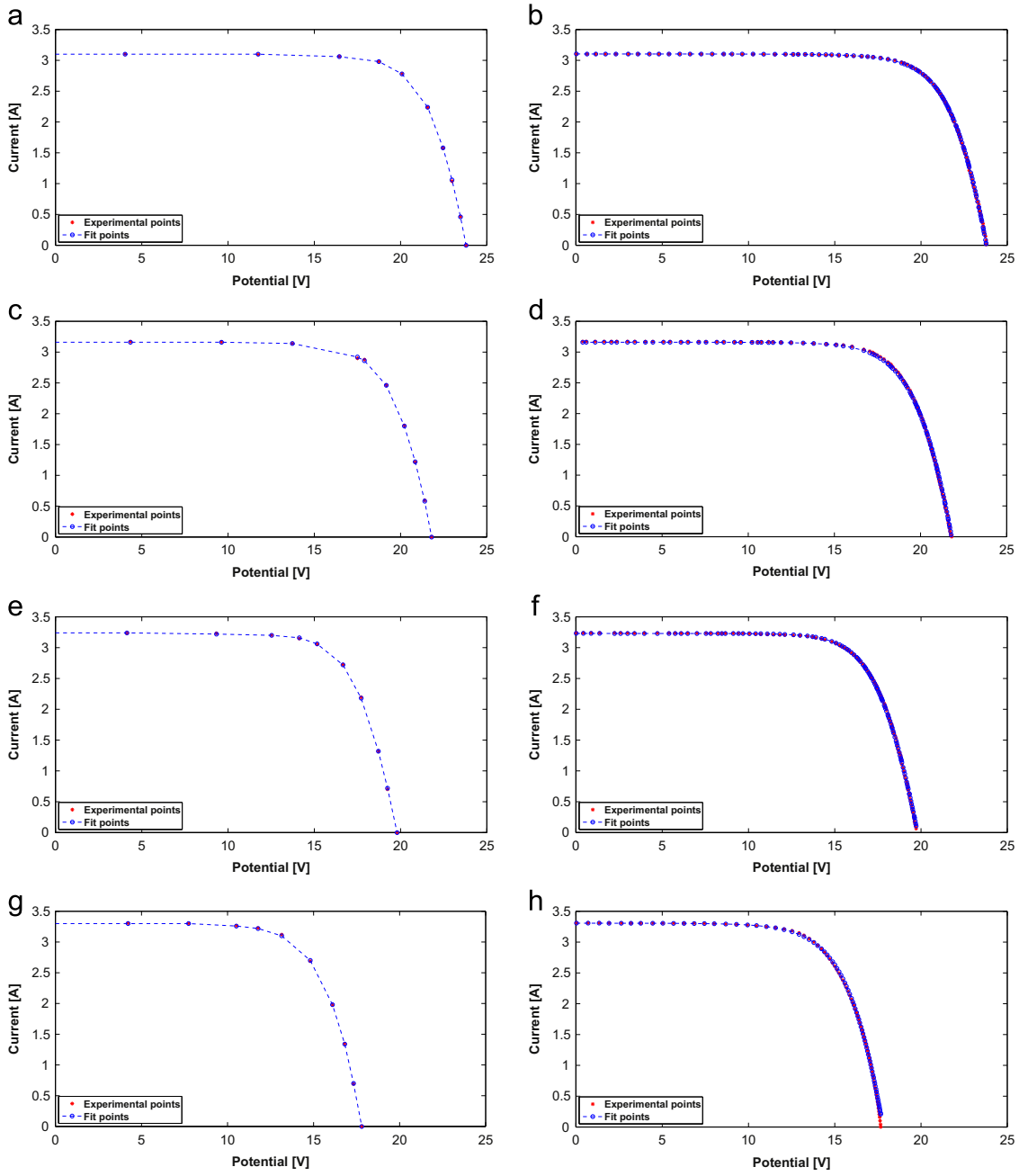

Fig. 4. Best fit parameters for the isothermal data by the double diode model (i.e. minimum values of Table 1). On the left side are the confrontations with the data used for the optimization, $data_f^{optim}$, and on the right side are confrontations with the data points used to verify the parameters that were found, $data_f^{check}$. Values from Tables 1 and 2 are reminded here in the sub-captions. (a) $X_{fit}(\Theta_{0\,^\circ C}^{(2)}, data_{0\,^\circ C}^{optim}) = 0.5$ cA/point. (b) $X_{fit}(\Theta_{0\,^\circ C}^{(2)}, data_{0\,^\circ C}^{check}) = 1.0$ cA/point. (c) $X_{fit}(\Theta_{25\,^\circ C}^{(2)}, data_{25\,^\circ C}^{optim}) = 0.9$ cA/point. (d) $X_{fit}(\Theta_{25\,^\circ C}^{(2)}, data_{25\,^\circ C}^{check}) = 1.7$ cA/point. (e) $X_{fit}(\Theta_{50\,^\circ C}^{(2)}, data_{50\,^\circ C}^{optim}) = 0.7$ cA/point. (f) $X_{fit}(\Theta_{50\,^\circ C}^{(2)}, data_{50\,^\circ C}^{check}) = 1.2$ cA/point. (g) $X_{fit}(\Theta_{75\,^\circ C}^{(2)}, data_{75\,^\circ C}^{optim}) = 0.6$ cA/point. (h) $X_{fit}(\Theta_{75\,^\circ C}^{(2)}, data_{75\,^\circ C}^{check}) = 2.5$ cA/point.

After 20 statistical runs, the parameter extraction concerning the four temperatures optimized at the same time was actually expected to bear more physical meaning than in the case of the different isothermal curves taken separately. Yet, with a zero value series resistor in the optimum of Table 4, this is contradictory. The physical meaning behind the series resistance is indeed depending on the ohmic resistance of the silver bus bars collecting the charge carriers from the whole solar cell, which is a major source for R_s [3], and then cannot be zero.

To explain this zero resistor within the optimization techniques undertaken in this study, we interpret that the high number of parameters for the diode models induce a transfer of physical meaning from one equivalent electrical component to the other. For example, the series resistor could be transferred to a loss of potential into the diode dark current. The same behavior could also happen with the parallel resistor taking high values, thus transferring the shunt resistance effect towards a loss of generated photocurrent (we note that this is also apparently happening for our optimums here).

To mitigate to some extend these trends, the optimizing scheme should rely on more constrained relations than the ones found only in the manufacturer datasheet. This can be done for example by relying on more illumination conditions in addition to the temperature effect. This can also be done by extending the *I–V*

Table 3
Comparison of performance between PSO, GA, CS and CS-NMS algorithms for parameters of the single and two-diode models. The values give the minimal, average, standard and maximal error in cA/point. The unique best values are underlined.

PSO				GA				CS				CS-NMS		
Min	Avg(Std)	Max	⋮	Min	Avg(Std)	Max	⋮	Min	Avg(Std)	Max	⋮	Min	Avg(Std)	Max
One-diode (10 parameters, i.e. for all $\Xi^{(1)}$)														
7.9	26.4(17.4)	60.5	⋮	12.0	16.1(3.2)	22.0	⋮	8.3	10.7(0.7)	11.6	⋮	9.7	11.1(0.8)	12.5
Two-diode (13 parameters, i.e. for all $\Xi^{(2)}$)														
13.6	28.6(14.6)	61.9	⋮	7.7	22.2(9.0)	46.5	⋮	6.6	6.9(0.3)	7.5	⋮	6.7	7.5(0.9)	10.1

Table 4
Values of the parameters for the best result of PSO and of CS that was more consistent. These are 10-parameter sets ($\Xi^{(1)}$) for the single diode model. ‡ are values at any border of the search space.

Parameter	CS	PSO	Units
$I_{ph,Ref}$	1.584000	1.589399	A
$\mu_{I_{sc}}$	1.500000e−03 ‡	1.129952e−03	A/°C
E_A	1.386187e−19	1.717348e−19	J
I_{00}	7.256565e+08	5.803972e+10	A
$A_{0,Ref}$	1.746305	1.381147	at 311 K
a	0.420093	0.4323318	
R_{s0}	0 ‡	1.66969e−2	Ω
B_s	0 ‡	8.840109e−6	K^{-1}
R_{p0}	10,000 ‡	9.563144e+3	Ω
B_p	1100 ‡	5.844332e+2	K
$X_{fit}(data^{optim}) =$	8.3	7.9	cA/point
$X_{fit}(data^{check}) =$	9.2	8.7	cA/point

Table 5
Values of parameters for the best result found by CS in case of the 13 parameters $\Xi^{(2)}$ fitting, for double diode model. See also Fig. 5. ‡ are values at any border of the search space.

Parameter	Value	Units
$I_{ph,Ref}$	1.582675	A
$\mu_{I_{sc}}$	1.487288e−03	A/°C
E_A	1.413473e−19	J
$I_{00;1}$	9.638854e+08	A
$A_{0;1}$	1.707615	at 311 K
$a^{(1)}$	0.4000101	
$I_{00;2}$	0 ‡	A
$A_{0;2}$	6.857028	at 311 K
$a^{(2)}$	0.400000 ‡	
R_{s0}	7.702958e−03	Ω
B_s	1.338306e−04	K^{-1}
R_{p0}	10,000 ‡	Ω
B_p	667.5793	K
$X_{fit}(data^{optim}) =$	6.6	cA/point
$X_{fit}(data^{check}) =$	7.6	cA/point

model by using it outside the first quadrant, relevant for solar power production. These propositions of adding more constraints can be applied without having too much to change within the theoretical background of the diode models.

Nevertheless, the best parameters reported in this section are very accurately describing the experimental anisothermal *I–V* curves behaviors. Thus, they can be used to predict the electrical response at any temperature. The observed shifting phenomenon leads to less pertinent values of the electrical components of the diode equivalent circuits, but altogether they have a correct behavior relatively to this application. It can be noted that we could also reverse our approach as it was done for the parameters in the short case study, i.e. fixing parameters to physical measurements or/and more empirical relations establishing physically meaningful order of magnitude for the parameters under study. However, even if by doing so we can constrain the system to avoid a zero resistor optimum, it does not imply that the same kind of shifting is prohibited between the loose parameters (this shift being then also less evident to highlight).

From the illustration of the best optimum found by the two-diode models (which could be a one-diode model) in Fig. 5, it can be noted that the fitting is not well done around P_{Max} for the highest temperature (75 °C). Still, the fitness function is globally correct for the 75 °C *I–V* characteristic, evaluated with the multi-*T* parameters around 9.0 and 9.4 cA/point respectively for the one- and two-diode optimums (for the $data^{optim}_{75\ °C}$ points only). If this kind

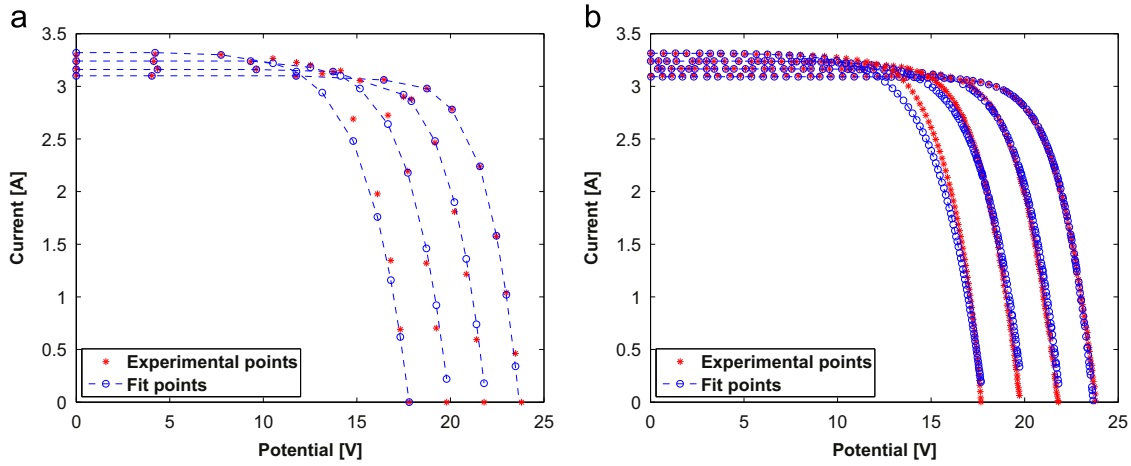

Fig. 5. Results for the best run of the double diode model for fitting parameters over all the temperatures at the same time. Fitness function values are given in the different sub-captions. (a) Optimization data set, $X_{fit}(\Xi^{(2)}, data^{optim}) = 6.6$ cA/point. (b) Check data set, $X_{fit}(\Xi^{(2)}, data^{check}) = 7.6$ cA/point.

of apparent misfit is problematic, more points of $data^{optim}$ could be taken near the four different P_{Max}, or only near this $P_{Max}(75\ ^{\circ}C)$ specifically, in order to try enhancing the fitting at these maximum power points.

5. Conclusion

Using evolutionary algorithms, the electrical parameter extraction for PV panel current–voltage (I–V) characteristics is easy to undertake with the one- or two-diode equivalent circuit formalism.

These models enable us to find good electrical parameters using the experimental standard data available in any PV panel manufacturer datasheet. It is possible to extract the diode models parameters for different available isothermal I–V characteristics, but it is also possible to take the curves as a whole set to fit simultaneously, by expressing explicit thermal-dependence of the diode models.

Taking the whole set of experimental I–V characteristics and the semi-empirical relations we used, the optimum fitting parameters reported in Table 5 is a set very reliable to define the thermal-dependence of the electrical response for this PV device.

However, letting the parameters have too many degrees of freedom within the search space seems to suppress some of the physical meaning of these parameters by the optimization (fitting) process. Further refinements of the proposed approach should include more solar irradiance dependance and/or firmer physical grounding of the diode models, especially outside the first quadrant such as in shaded service conditions.

The photocurrent could also come for example directly from the photon energy distribution with an absorption efficiency and balanced by other constraints due to common impediments to the solar conversion. Fixing the photocurrent in this way during the optimization scheme applied to the parameters' extraction may avoid the observed drifting of counterbalanced electrical components towards non-physical values authorized within the diode models search space.

Anyway, the electrical behavior of all these parameters/circuit components, taken together, is what is important here, and it allows us to reach the objective of extrapolating I–V curves to a broad range of possible PV cell operating temperatures.

Acknowledgments

Dr. J.P.M. Correia and J.C. Sánchez Barroso from ICube Laboratory, University of Strasbourg–CNRS, France, are gratefully acknowledged for collaboration and support of an initial work in the domain of the extraction of PV cell electrical parameters, as well as for fruitful discussions concerning the thermal management and temperature effects in the PV panels.

Appendix A. Short case study, additional equations

In a previous study [15], we reduced parameters of the search space of the presented 5-parameter single diode model. For this particular purpose, the relations listed below were used to replace some of the 5 mentioned parameters with the following semi-empirical relations, and also with eventual measurements. It should be noted that these expressions are associated to the BP 350 U PV panel. The fitness function J_{fit} at this time is also given below in Eq. (A.4):

$$I_{ph} = I_{SC} \tag{A.1}$$

where I_{SC} is the short circuit current at the cell level (as the panel has two parallel strings of PV cells, this current is the half the one of the panel):

$$I_0 = \frac{I_{SC}}{\exp\left(\frac{q \times V_{OC}}{k_B \times A \times T}\right) - 1} \tag{A.2}$$

where V_{OC} is at the cell level which equals the one at the panel level but divided by 36 (as the panel has 36 PV cells in each of the parallel strings); and the ideality factor A is taken at

$$A = 1.025 \text{ for polycrystalline silicon solar cells} \tag{A.3}$$

$$J_{fit}(Rs, Rp, I_{SC}, P_{Max}, V_{OC}) = \sum_{I_k \in \left\{I_{SC}, I_{P_{Max}}, I_{V_{OC}} = 0\right\}} (I_k - I_{calc,k})^2 + \left|\frac{\partial P_{calc,Max}}{\partial U}\right|_{U_{P_{Max}}} \tag{A.4}$$

Appendix B. Supplementary data

Supplementary data associated with this article can be found in the online version at http://dx.doi.org/10.1016/j.solmat.2015.09.003.

References

[1] D.L. King, J.A. Kratochvil, W.E. Boyson, Photovoltaic Array Performance Model, Sandia Report SAND2004-3535, Department of Energy, Sandia National

Laboratories, United States, 2004, 43 pp. (URL ⟨http://prod.sandia.gov/techlib/access-control.cgi/2004/043535.pdf⟩).
[2] J. Sánchez Barroso, N. Barth, J. Correia, S. Ahzi, M. Khaleel, A computational analysis of coupled thermal and electrical behavior of PV panels, Sol. Energy Mater. Sol. Cells 148 (2016) 73–86, http://dx.doi.org/10.1016/j.solmat.2015.09.004.
[3] T. Dittrich, Materials concepts for solar cells, in: Energy Futures, vol. 1, Imperial College Press, 2014, 552 pp., ISBN:978-1783264452, 57 Shelton Street, Covent Garden, London WC2H 9HE, England http://dx.doi.org/10.1142/p937.
[4] A. Slaoui, Électricité photovoltaïque – Principes, Éditions Techniques de l'Ingénieur traité Génie énergétique, 2013, BE8578v2.1–14 (in French).
[5] D. Chan, J. Phang, Analytical methods for the extraction of solar-cell single- and double-diode model parameters from *I*–*V* characteristics, IEEE Trans. Electron. 34 (2) (1987) 286–293, http://dx.doi.org/10.1109/T-ED.1987.22920.
[6] M. Wolf, G. Noel, R.J. Stirn, Investigation of the double exponential in the current–voltage characteristics of silicon solar cells, IEEE Trans. Electron. Devices 24 (4) (1977) 419–428, http://dx.doi.org/10.1109/T-ED.1977.18750.
[7] M. Ye, X. Wang, Y. Xu, Parameter extraction of solar cells using particle swarm optimization, J. Appl. Phys. (Melville, NY, U.S.) 105 (9) (2009) (094502.1–8. http://dx.doi.org/10.1063/1.3122082).
[8] N. Moldovan, R. Picos, E. Garcia-Moreno, Parameter extraction of a solar cell compact model using genetic algorithms, in: 2009 Spanish Conference on Electron Devices, CDE 2009, 2009, pp. 379–382. http://dx.doi.org/10.1109/SCED.2009.4800512.
[9] Y.-P. Chang, Optimal the tilt angles for photovoltaic modules using PSO method with nonlinear time-varying evolution, Energy 35 (5) (2010) 1954–1963, http://dx.doi.org/10.1016/j.energy.2010.01.010.
[10] H. Qin, J. Kimball, Parameter determination of photovoltaic cells from field testing data using particle swarm optimization, in: 2011 IEEE Power and Energy Conference at Illinois, PECI, 2011, pp. 1–4. http://dx.doi.org/10.1109/PECI.2011.5740496.
[11] J. Ma, T. Ting, K.L. Man, N. Zhang, S.-U. Guan, P.W. Wong, Parameter estimation of photovoltaic models via cuckoo search, J. Appl. Math. 2013 (2013) (362619.1–8. http://dx.doi.org/10.1155/2013/362619).
[12] M. Siddiqui, M. Abido, Parameter estimation for five- and seven-parameter photovoltaic electrical models using evolutionary algorithms, Appl. Soft Comput. 13 (12) (2013) 4608–4621, http://dx.doi.org/10.1016/j.asoc.2013.07.005.
[13] N. Krishnakumar, R. Venugopalan, N. Rajasekar, Bacterial foraging algorithm based parameter estimation of solar PV model, in: 2013 Annual International Conference on Emerging Research Areas and 2013 International Conference on Microelectronics, Communications and Renewable Energy, AICERA/ICMiCR, 2013, pp. 1–6. http://dx.doi.org/10.1109/AICERA-ICMiCR.2013.6575948.
[14] N. Tutkun, E. Elibol, D. Maden, Basic parameter extraction from an organic solar cell through the single diode model and a metaheuristic technique with the Lambert W function, in: 2014 International Renewable and Sustainable Energy Conference, IRSEC, 2014, pp. 554–558. http://dx.doi.org/10.1109/IRSEC.2014.7059778.
[15] J. Sánchez Barroso, J. Correia, N. Barth, S. Ahzi, M. Khaleel, A PSO algorithm for the calculation of the series and shunt resistances of the PV panel one-diode model, in: 2014 International Renewable and Sustainable Energy Conference, IRSEC, 2014, pp. 1–6. http://dx.doi.org/10.1109/IRSEC.2014.7059883.
[16] D. Gokilapriya, S. Barvin Banu, MPPT measurement of photovoltaic system under partial shading condition using DPSO algorithm, in: C. Kamalakannan, L. P. Suresh, S.S. Dash, B.K. Panigrahi (Eds.), Power Electronics and Renewable Energy Systems, Lecture Notes in Electrical Engineering, vol. 326, Springer, India, 2015, pp. 1037–1046, http://dx.doi.org/10.1007/978-81-322-2119-7_101.
[17] Vandana Khanna, B.K. Das, Dinesh Bisht, P.K. Singh, A three diode model for industrial solar cells and estimation of solar cell parameters using PSO algorithm, Renew. Energy 78 (2015) 105–113, http://dx.doi.org/10.1016/j.renene.2014.12.072.
[18] W. De Soto, S. Klein, W. Beckman, Improvement and validation of a model for photovoltaic array performance, Sol. Energy 80 (1) (2006) 78–88, http://dx.doi.org/10.1016/j.solener.2005.06.010.
[19] R. Khezzar, M. Zereg, A. Khezzar, Modeling improvement of the four parameter model for photovoltaic modules, Sol. Energy 110 (2014) 452–462, http://dx.doi.org/10.1016/j.solener.2014.09.039.
[20] BP Solar, BP 350 U—50 Watt Photovoltaic Module Datasheet, June 2014, Available from ⟨http://midsummerenergy.co.uk/pdfs/BP_50W_datasheet.pdf⟩, 2004.
[21] S. Astier, Conversion photovoltaïque: du rayonnement solaire à la cellule, Éditions Techniques de l'ingénieur Optique Photonique, Électronique – Automatique, 2008, D3935.1–20 (in French).
[22] H.-L. Tsai, Complete PV model considering its thermal dynamics, J. Chin. Inst. Eng. 36 (8) (2013) 1073–1082, http://dx.doi.org/10.1080/02533839.2012.747044.
[23] M.U. Siddiqui, A. Arif, L. Kelley, S. Dubowsky, Three-dimensional thermal modeling of a photovoltaic module under varying conditions, Sol. Energy 86 (9) (2012) 2620–2631, http://dx.doi.org/10.1016/j.solener.2012.05.034.
[24] J. Ding, X. Cheng, T. Fu, Analysis of series resistance and *P*–*T* characteristics of the solar cell, Vacuum 77 (2) (2005) 163–167, http://dx.doi.org/10.1016/j.vacuum.2004.08.019.
[25] S. Bensalem, M. Chegaar, Thermal behavior of parasitic resistances of polycrystalline silicon solar cells, Rev. Énerg. Renouv. 16 (1) (2013) 171–176 (URL ⟨http://www.cder.dz/download/Art16-115.pdf⟩).
[26] R. Jovanovic, S. Kais, F.H. Alharbi, Cuckoo search inspired hybridization of the Nelder-Mead simplex algorithm applied to optimization of photovoltaic cells, submitted for publication, Appl. Math. Inf. Sci. 10 (3) (2016) arXiv:1411.0217.
[27] X.-S. Yang, Cuckoo Search (CS) Algorithm (computer software) ⟨http://www.mathworks.com/matlabcentral/fileexchange/29809-cuckoo-search–cs–algorithm⟩, February 2013.
[28] R. Jovanovic, Nelder–Mead Hybridization of Cuckoo Search (computer software) ⟨http://www.mathworks.com/matlabcentral/fileexchange/46789-nelder-mead-hybridization-of-cuckoo-search⟩, May 2014.
[29] M. Siddiqui, A. Arif, A. Bilton, S. Dubowsky, M. Elshafei, An improved electric circuit model for photovoltaic modules based on sensitivity analysis, Sol. Energy 90 (2013) 29–42, http://dx.doi.org/10.1016/j.solener.2012.12.021.
[30] H. Bayhan, A.S. Kavasoglu, Exact analytical solution of the diode ideality factor of a pn junction device using Lambert W-function model, Turk. J. Phys. 31 (1) (2007) 7–10 (URL ⟨http://mistug.tubitak.gov.tr/bdyim/abs2.php?dergi=fiz&rak=0609-3⟩).
[31] R. Eberhart, Y. Shi, Particle swarm optimization: developments, applications and resources, in: Proceedings of the 2001 Congress on Evolutionary Computation, vol. 1, 2001, pp. 81–86. http://dx.doi.org/10.1109/CEC.2001.934374.
[32] X.-S. Yang, S. Deb, Cuckoo search via Lévy flights, in: World Congress on Nature & Biologically Inspired Computing, NaBIC 2009, IEEE, 2009, pp. 210–214. http://dx.doi.org/10.1109/NABIC.2009.5393690.
[33] X.-S. Yang, S. Deb, Engineering optimisation by cuckoo search, Int. J. Math. Model. Numer. Optim. 1 (4) (2010) 330–343, http://dx.doi.org/10.1504/IJMMNO.2010.03543.
[34] X.-S. Yang, S. Deb, Cuckoo search: recent advances and applications, Neural Comput. Appl. 24 (1) (2014) 169–174, http://dx.doi.org/10.1007/s00521-013-1367-1.
[35] A. Gandomi, X.-S. Yang, A. Alavi, Cuckoo search algorithm: a metaheuristic approach to solve structural optimization problems, Eng. Comput. 29 (1) (2013) 17–35, http://dx.doi.org/10.1007/s00366-011-0241-y.